

LOW FREQUENCY CAPACITANCE MEASUREMENTS OF THE AGS BOOSTER ELECTROSTATIC PICK-UP ELECTRODES

D. J. Ciardullo

September 1990

Collider Accelerator Department
Brookhaven National Laboratory

U.S. Department of Energy
USDOE Office of Science (SC)

Notice: This technical note has been authored by employees of Brookhaven Science Associates, LLC under Contract No. DE-AC02-76CH00016 with the U.S. Department of Energy. The publisher by accepting the technical note for publication acknowledges that the United States Government retains a non-exclusive, paid-up, irrevocable, world-wide license to publish or reproduce the published form of this technical note, or allow others to do so, for United States Government purposes.

DISCLAIMER

This report was prepared as an account of work sponsored by an agency of the United States Government. Neither the United States Government nor any agency thereof, nor any of their employees, nor any of their contractors, subcontractors, or their employees, makes any warranty, express or implied, or assumes any legal liability or responsibility for the accuracy, completeness, or any third party's use or the results of such use of any information, apparatus, product, or process disclosed, or represents that its use would not infringe privately owned rights. Reference herein to any specific commercial product, process, or service by trade name, trademark, manufacturer, or otherwise, does not necessarily constitute or imply its endorsement, recommendation, or favoring by the United States Government or any agency thereof or its contractors or subcontractors. The views and opinions of authors expressed herein do not necessarily state or reflect those of the United States Government or any agency thereof.

LOW FREQUENCY CAPACITANCE MEASUREMENTS OF THE
AGS BOOSTER ELECTROSTATIC PICK-UP ELECTRODES

BOOSTER TECHNICAL NOTE
NO. 178

D. J. CIARDULLO

SEPTEMBER 13, 1990

ALTERNATING GRADIENT SYNCHROTRON DEPARTMENT
BROOKHAVEN NATIONAL LABORATORY
UPTON, NEW YORK 11973

LOW FREQUENCY CAPACITANCE MEASUREMENTS OF THE AGS BOOSTER ELECTROSTATIC PICK-UP ELECTRODES

INTRODUCTION

Capacitance measurements have been made on a typical Booster production PUE assembly. The detector is the split cylinder electrostatic type, which provides plate signals linearly related to the transverse position of the beam¹. A fundamental difference between this and other split cylinder detectors, however, is the addition of a "calibration ring" which encircles both PUEs. The ring simulates a centered beam by coupling an applied input signal equally to both plates (this is useful for doing limited BPM system diagnostics without actually requiring beam). There is, however, an overall decrease in both the common mode and differential detector sensitivities, since the capacitances related to the calibration ring act parasitic to the electrodes. The detector and its associated capacitances are shown in Figure 1.

The purpose of this technical note is to obtain the value of each "isolated" capacitance element of the detector model shown in Figure 2:

| | | |
|----------|---|---|
| C_{pp} | : | Plate to plate capacitance |
| C_{pc} | : | Plate to calibration ring capacitance |
| C_p | : | Plate to detector shell capacitance |
| C_c | : | Calibration ring to shell capacitance |
| C_f | : | Vacuum feedthru N-type connector (to shell) |

As can be seen from Figure 2, interactions due to coupling between the PUEs and the calibration ring make it difficult to measure any one isolated capacitance directly. However, a sufficient amount of information can be obtained by measuring specific element combinations. These "effective capacitances", described by the sub-models shown in Figures 3-5, can then be used to extract the isolated element values listed above.

EXTRACTION OF ISOLATED CAPACITANCES:

On a completed detector assembly, the capacitance measurements which can be made directly are:

| | |
|----------------------|---|
| $C_p(\text{eff})$ | The effective PUE to shell capacity, looking into the electrode feedthru, |
| $C_c(\text{eff})$ | the effective calibration ring to shell capacity, looking into one of the calibration ring feedthrus, and |
| $C_{pp}(\text{eff})$ | the effective inter-electrode capacity, as measured between the center conductors of both electrode vacuum feedthrus. |

The term "effective" is used since each reading results from a different combination of all the capacitances within the detector (refer to Fig. 2).

These three measurement values provide insufficient information to completely determine the detector model of Figure 2. Additional measurements are needed which require partial disassembly of the detector.

DETERMINING C_r

First, mechanically separable components are removed from the assembly (elements in Figure 2 represented by dashed lines). These components include the vacuum feedthru connectors, as well as any external load on the calibration ring or the plates. Once isolated, the capacitance of each detached component is easily measured.

DETERMINING C_{pp} AND C_{pc} :

The second group of capacitance readings were taken on the subassembly formed by the split cylinder and the calibration ring outside of the detector shell (see figure 3). The measurements obtained from this subassembly are:

$$C_{pp}(\text{eff}) = C_{pp} + \frac{C_{pc}}{2} \quad (1)$$

$$C_{pc}(\text{eff}) = C_{pc} + \frac{C_{pc} C_{pp}}{C_{pc} + C_{pp}} \quad (2)$$

where $C_{pp}(\text{eff})$ is the effective capacitance as measured across the plates (electrodes), and $C_{pc}(\text{eff})$ is the effective capacitance from one plate to the calibration ring. Note that these values are the result of specific combinations of the capacitance elements shown in Figure 3 (lower case subscripts will be used to distinguish measurements made on subassemblies from those made on a completely assembled detector).

Equations (1) and (2) can be used to extract the element values for C_{pp} and C_{pc} from their measured "effective" capacitances:

$$C_{pp} = C_{pp}(\text{eff}) \left[1 - \frac{C_{pc}(\text{eff})}{4 C_{pp}(\text{eff}) - C_{pc}(\text{eff})} \right] \quad (3)$$

$$C_{pc} = 2 \frac{C_{pp}(\text{eff}) C_{pc}(\text{eff})}{4 C_{pp}(\text{eff}) - C_{pc}(\text{eff})} \quad (4)$$

DETERMINING C_p AND C_c :

The last group of readings are taken on the detector assembly, less any vacuum feedthru connectors (or other external load). The measurements obtained from this assembly are (refer to Figures 4 and 5):

$$C_p(\text{eff}) = C_p + \frac{C_{pc} C_c}{C_c + 2 C_{pc}} + \frac{1}{\frac{1}{C_{pp} + \frac{C_{pc}^2}{C_c + 2 C_{pc}}} + \frac{1}{C_p + \frac{C_{pc} C_c}{C_c + 2 C_{pc}}}} \quad (5)$$

$$C_c(\text{eff}) = C_c + \frac{C_{pc} C_p}{C_p + C_{pp} + C_{pc}} + \frac{1}{\frac{1}{C_{pc} + \frac{C_{pc} C_{pp}}{C_p + C_{pp} + C_{pc}}} + \frac{1}{C_p + \frac{C_p C_{pp}}{C_p + C_{pp} + C_{pc}}}} \quad (6)$$

where C_{pp} and C_{pc} are calculated from equations (3) and (4). Figures 4 and 5 illustrate the capacitive elements which make up $C_p(\text{eff})$ and $C_c(\text{eff})$, respectively. Note that "wye-delta" impedance transformations are used to simplify both submodels. The general wye-delta transformation is shown in Appendix 1.³

Values for C_p and C_c have been extracted from equations (5) and (6) using the program MACSYMA. Appendix 2 shows the solution for C_p in terms of C_{pp} , C_{pc} and the measured "effective" capacitances. Once C_p has been determined, eq. (6) is used to solve for the calibration ring capacitance, C_c .

ACTUAL MEASUREMENT VALUES:

The following effective capacitance readings were taken on a "typical" production electrostatic detector (S/N 039):

| | | |
|----------------------|---|-------|
| C_f | : | 7 pF |
| $C_{pp}(\text{eff})$ | : | 24 pF |
| $C_{pc}(\text{eff})$ | : | 17 pF |
| $C_p(\text{eff})$ | : | 45 pF |
| $C_c(\text{eff})$ | : | 56 pF |

These measurements were taken with an HP4262A LCR meter. C_f is an actual element in the detector model of Figure 2; the remaining components in the model can now be calculated using eq. (3), (4), (6) and Appendix 2. The following values result:

| | | | |
|----------|---|---------|-------------------------|
| C_{pp} | = | 18.8 pF | |
| C_{pc} | = | 10.3 pF | |
| C_p | = | 25.6 pF | |
| C_c | = | 41.3 pF | |
| C_f | = | 7 pF | (by direct measurement) |

Figure 6 shows the capacitance model for the typical Booster average orbit electrostatic detector, with the actual element values listed. Note that the external load capacitance on each PUE ($C_L(p)$) depends on the BPM system gain, and can take one of two values (210 pF or 2610 pF). $C_L(c)$ is the capacitance loading due to the cable assembly connecting the calibration ring to the BPM electronics (approximately 285 pF at low frequencies).

EFFECTIVE PUE CAPACITANCE LOAD:

The effective electrode capacitance, $C_{pue}(\text{eff})$, is the load that the beam "sees" due to each PUE. This is defined by equation (7) below, which is equation (5) with the following modifications:

- . C_p replaced by $C_p + C_f + C_L(p)$
- . C_c replaced by $C_c + 2 C_f + C_L(c)$

These modifications are necessary to account for the capacitance of the vacuum feedthru connectors, as well as any external loading of the detector.

Capacitance the beam "sees" from each PUE:

$$C_{pue}(eff) = C'_p + \frac{C_{pc} C'_c}{C'_c + 2 C_{pc}} + \frac{1}{\frac{1}{C_{pp} + \frac{C_{pc}^2}{C'_c + 2 C_{pc}}} + \frac{1}{C'_p + \frac{C_{pc} C'_c}{C'_c + 2 C_{pc}}}} \quad (7)$$

$$\begin{aligned} \text{where} \quad C'_p &= C_p + C_f + C_L(p) \\ C'_c &= C_c + 2C_f + C_L(c) \end{aligned}$$

CONCLUDING REMARKS

A capacitance model of the Booster average orbit electrostatic detector has been presented in Figure 6. The values of the individual capacitive elements have been calculated from measurements made on specific detector subassemblies.

Equation (7) gives the effective capacitance load presented to the beam from each electrode. It includes the effects of the vacuum feedthrus, the loading of the BPM electronics front end, and the capacitance due to the system connecting cables.

It is interesting to note that large changes in the capacitance loading of the calibration ring have only a small effect on the value of $C_{pue}(eff)$. At low frequencies, this effect is reduced even further when the calibration ring is loaded with 50 ohms (after installation into the Booster). The 50 ohm load bleeds off any charge trying to accumulate on C'_c (i.e., the cal ring, its connecting cable and two vacuum feedthrus). This essentially eliminates the capacitance contribution from C'_c and equation (7) can be approximated by:

$$C_{pue}(eff) \sim C_p' + \frac{1}{\frac{1}{C_{pp}} + \frac{C_{pc}}{2}} + \frac{1}{C_p'} \quad (8)$$

$$= C_p' + \frac{1}{\frac{1}{24} + \frac{1}{C_p'}} \quad (9)$$

$$\begin{aligned} \text{with } C_p' &= C_p + C_f + C_{cable} + C_{fep} \\ &= 25.6 + 7 + 153 + \begin{cases} 50 \text{ (x1, x10 BPM system gains)} \\ 2450 \text{ (x0.1 BPM system gain)} \end{cases} \end{aligned}$$

(all values in pF)

Using equation (9), the calibration ring is found to contribute an increase of $C_{pue}(eff)$ of less than 2% for the X1 and X10 BPM system gain modes, and less than 0.2% for the x0.1 gain mode.

ACKNOWLEDGEMENT:

The assistance of R. Thomas in both the use of MACSYMA and the review of this technical note is gratefully acknowledged. In addition, the support given by J. Cupolo in making the actual detector measurements is much appreciated.

REFERENCES:

1. R. E. Shafer, Beam Position Monitoring, Brookhaven Instrumentation Workshop (1989).
2. G. R. Lambertson, "Electromagnetic Detectors", in Frontiers of Particle Beams; Observation, Diagnosis and Correction (M. Month, S. Turner, eds.), p.380. Springer-Verlag, New York (1989).
3. W. H. Hayt, Jr., J. E. Kemmerly, Engineering Circuit Analysis, third edition, New York: McGraw Hill, 1978.

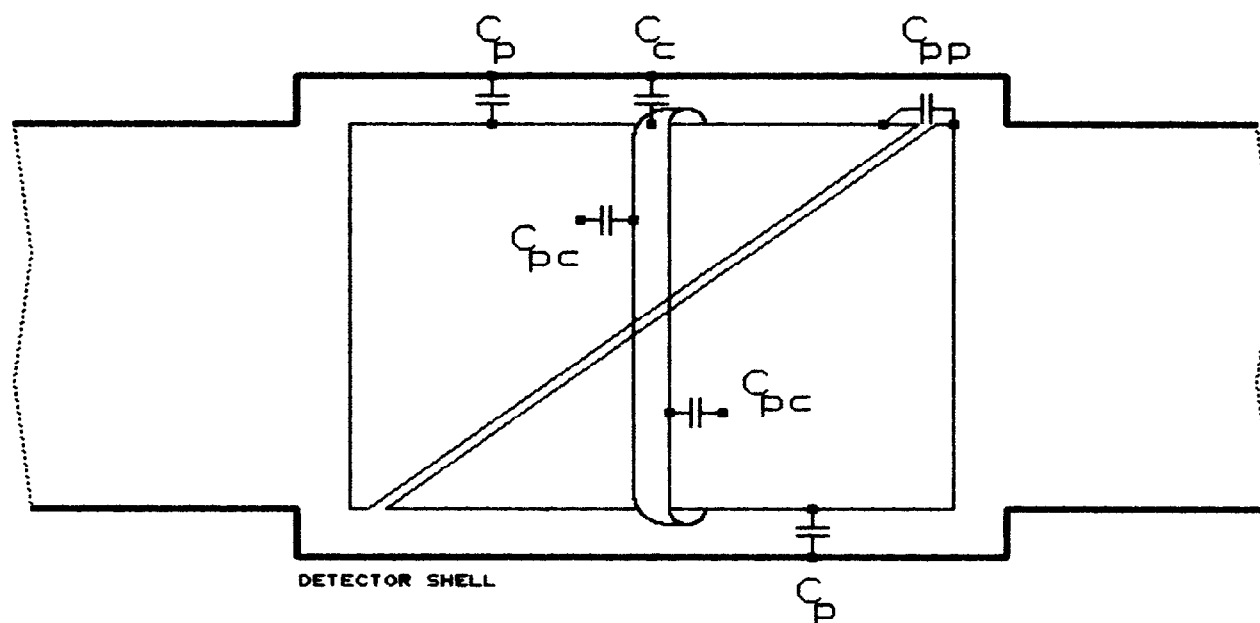
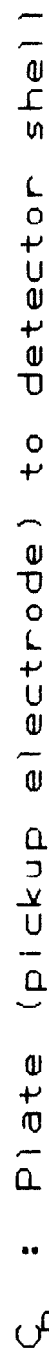


FIGURE 1. CAPACITANCES ASSOCIATED WITH THE BOOSTER ELECTROSTATIC PUE_s



Q_c : Calibration ring to detector shell

Copy: Plate to plate

C_{PC} : Plate to calibration ring

C_f : Vacuum feedthrough to detector shell

$Q_L(p)$: Any external capacitance load on the PUE

$Q_L(c)$: Any external capacitance load on the cal ring

FIGURE 2. GENERAL CAPACITANCE MODEL, BOOSTER ELECTROSTATIC PUE ASSY

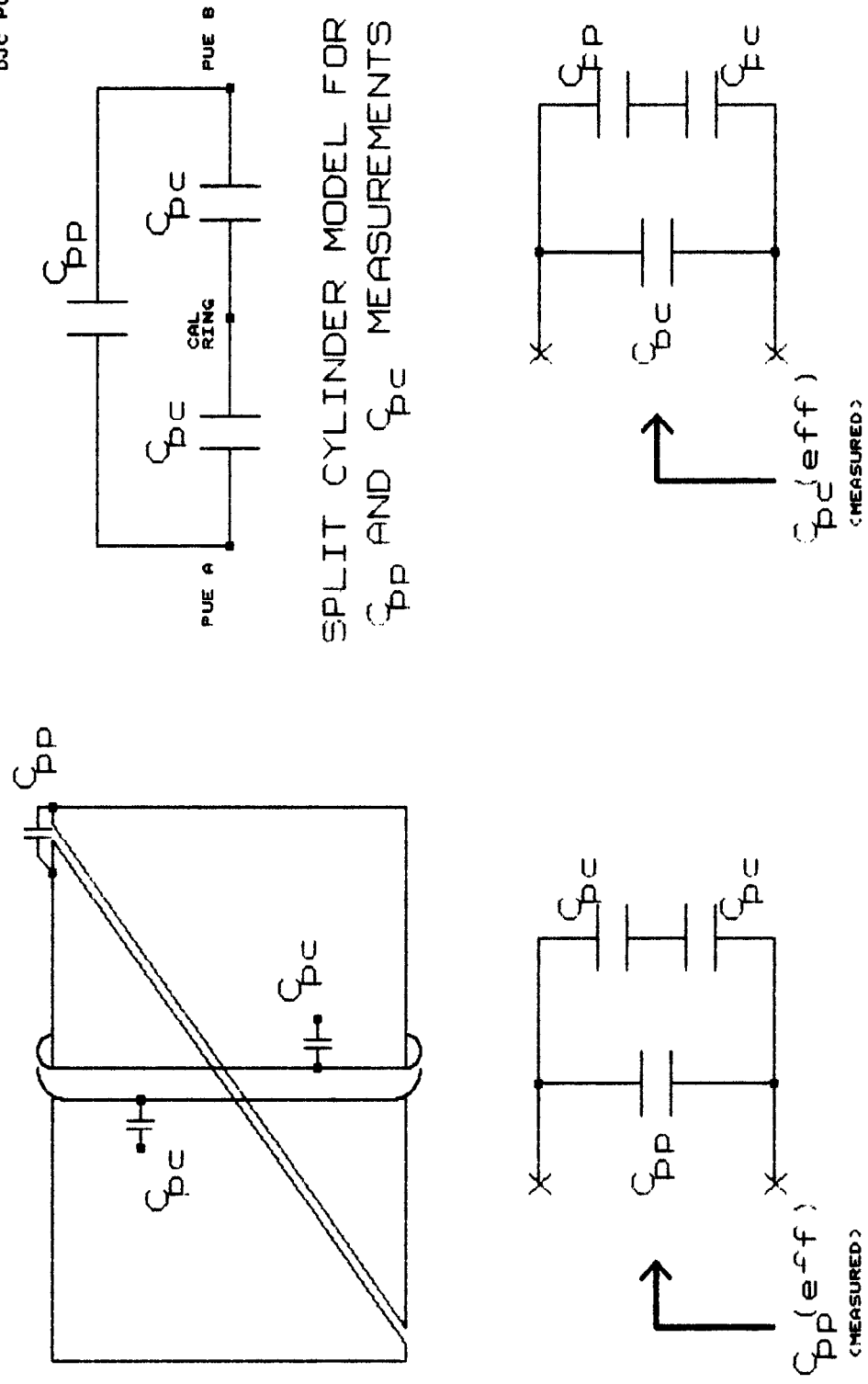
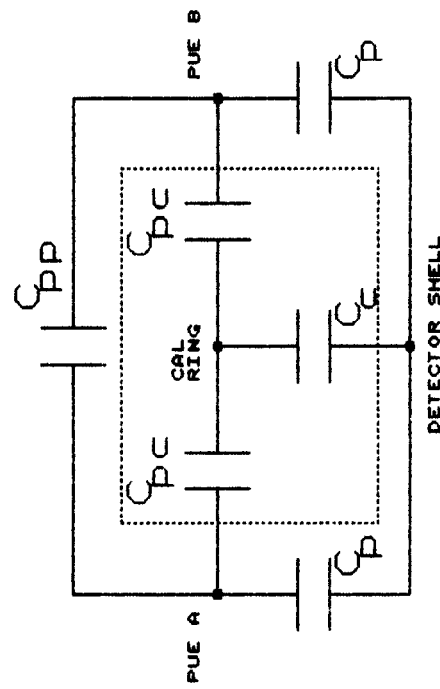
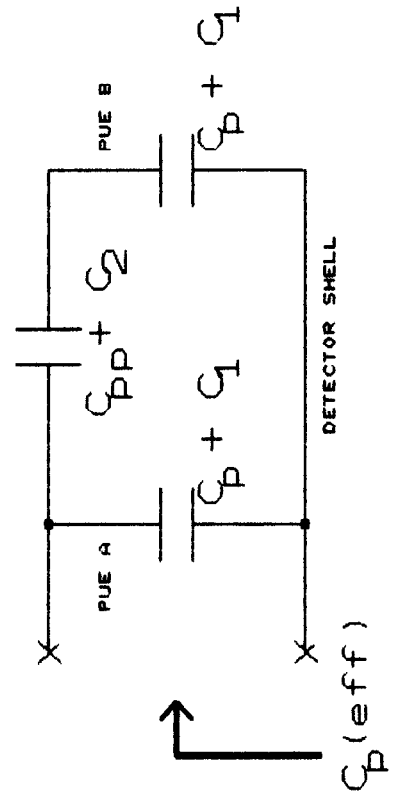
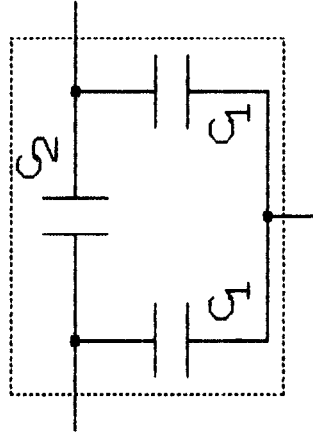


FIGURE 3. EFFECTIVE PLATE TO PLATE AND PLATE TO CAL RING CAPACITANCES



WYE-DELTA TRANSFORMATION OF
ELEMENTS WITHIN DASHED LINES
OF MODEL AT LEFT



$$C_1 = \frac{C_{pc} C_c}{C_c + 2C_{pc}} \quad C_2 = \frac{(C_{pc})^2}{C_c + 2C_{pc}}$$

ALL LOAD CAPACITANCES (i.e., feedthrus,
cables and front end electronics) ARE
LUMPED INTO C_p AND C_c .

FIGURE 4. EFFECTIVE ELECTRODE CAPACITANCE

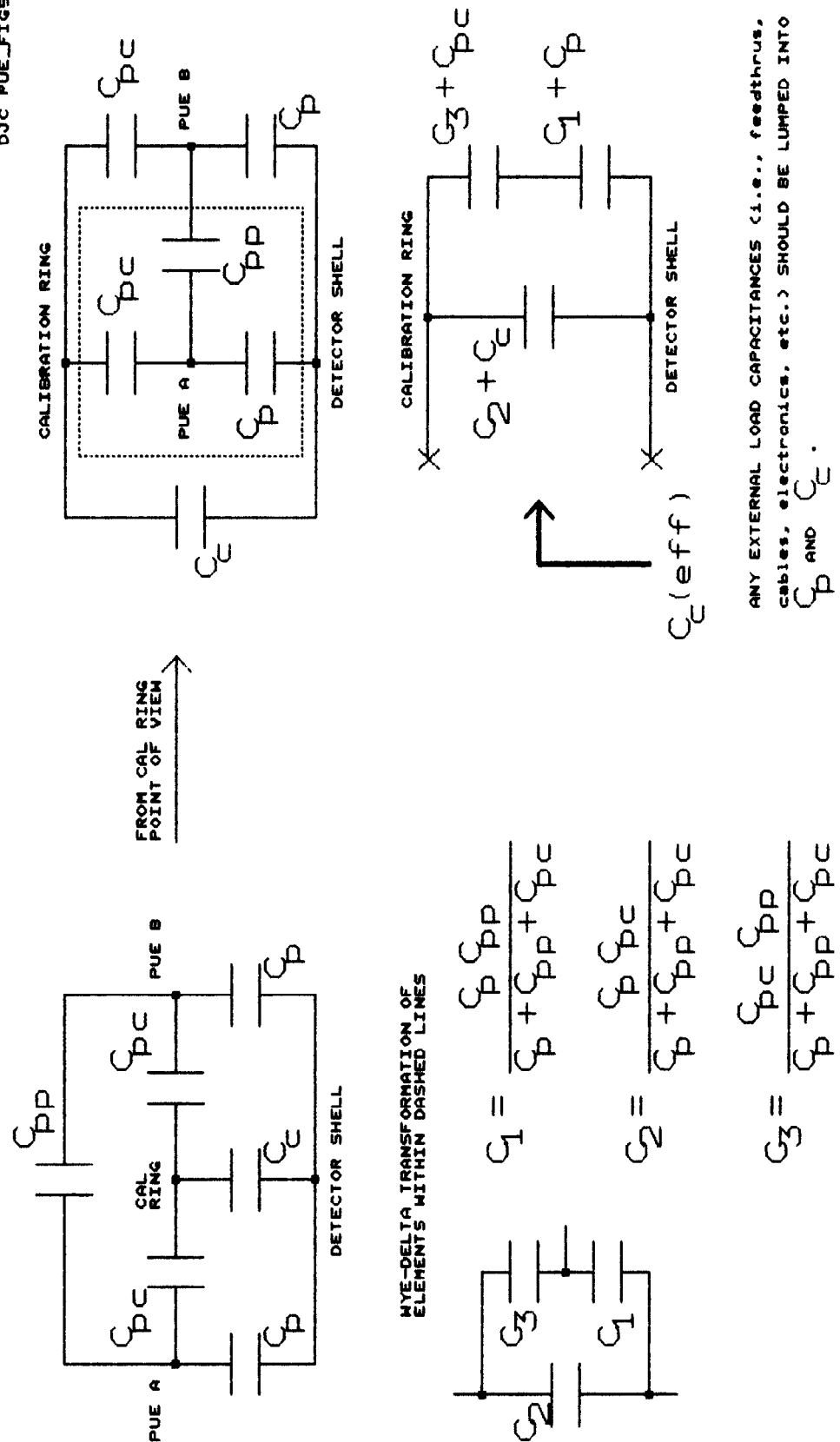
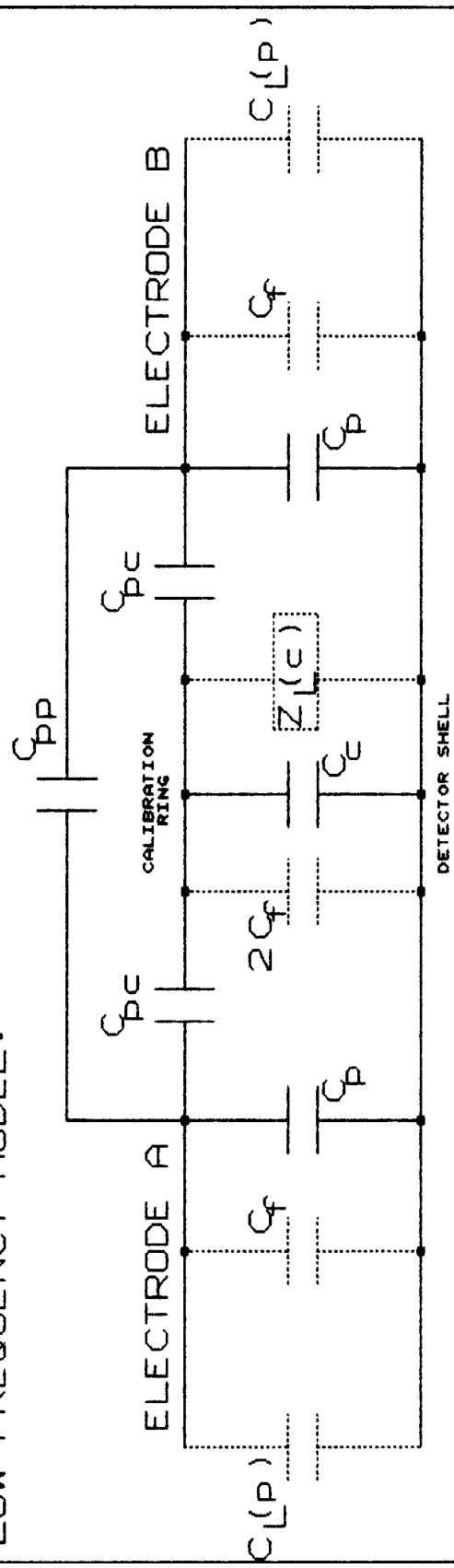


FIGURE 5. EFFECTIVE CAL RING CAPACITANCE

LOW FREQUENCY MODEL:



$$\begin{aligned}
 C_p &= 25.6 \text{ pF} \\
 C_c &= 41.3 \text{ pF} \\
 C_{pp} &= 18.8 \text{ pF} \\
 C_{pc} &= 10.3 \text{ pF} \\
 C_f &= 7.0 \text{ pF}
 \end{aligned}$$

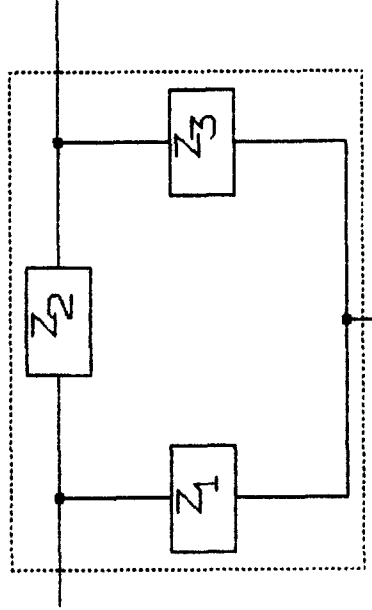
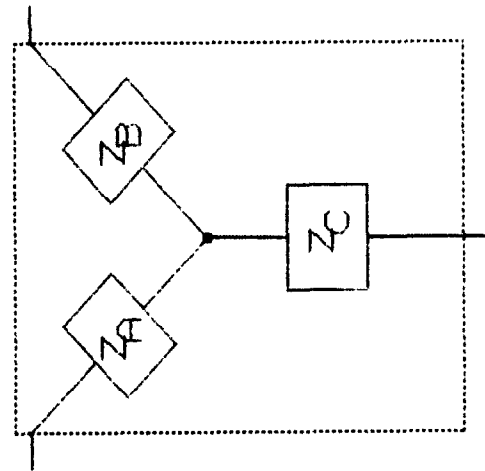
$$\begin{aligned}
 C_L(p) &= C_p + C_f + C_{cable} + C_{fep} \\
 &= 25.6 + 7.0 + 153 + 50 \text{ (x1, x10 modes)} \\
 &= 235.6 \text{ pF (x1, x10 modes)} \\
 &= 2635.6 \text{ pF (x10 mode)}
 \end{aligned}$$

$$Z_L(c) = 285 \text{ pF, shunted with } 50 \text{ ohms}$$

FIGURE 6. MODEL OF THE BOOSTER ELECTROSTATIC PUE ASSY, WITH FINAL ELEMENT VALUES

APPENDIX 1

WYE-DELTA IMPEDANCE TRANSFORMATION



$$Z_1 = Z_A + Z_C + \frac{Z_A Z_C}{Z_B} \longrightarrow G_1 = \frac{G_A G_C}{G_A + G_B + G_C}$$

$$Z_2 = Z_A + Z_B + \frac{Z_A Z_B}{Z_C} \longrightarrow G_2 = \frac{G_A G_B}{G_A + G_B + G_C}$$

$$Z_3 = Z_B + Z_C + \frac{Z_B Z_C}{Z_A} \longrightarrow G_3 = \frac{G_B G_C}{G_A + G_B + G_C}$$

APPENDIX 2

SOLUTION FOR C_p :

$$\begin{aligned}
 cp = & \text{expt}(\sqrt{-cpeff} \left[(4 cceff^3 cpeff + 64 cceff^2 cpc) cpp^4 \right. \\
 & - 16 cceff^2 cpc^2 cpeff cpp^3 + (cceff^3 cpeff^3 + 16 cceff^2 cpc^2 cpeff^2 \\
 & - 32 cceff cpc^4 cpeff) cpp^2 + (-6 cceff^2 cpc^2 cpeff^3 - 28 cceff cpc^4 cpeff^2) \\
 & \left. cpp + cceff cpc^4 cpeff^3 + 4 cpc^6 cpeff^2 \right] / cceff) / (6 \sqrt{3} cceff) \\
 & + (cceff (-16 cpp^3 + 6 cpeff cpp^2 - 3 cpeff^2 cpp + 2 cpeff^3) \\
 & + cpc^2 (36 cpeff cpp + 9 cpeff^2)) / (54 cceff), \frac{1}{3} \\
 & + (cceff (4 cpp^2 - cpeff cpp + cpeff^2) + 3 cpc^2 cpeff) \\
 & / (9 cceff \text{expt}(\sqrt{-cpeff} ((4 cceff^3 cpeff + 64 cceff^2 cpc) cpp^4 \\
 & - 16 cceff^2 cpc^2 cpeff cpp^3 + (cceff^3 cpeff^3 + 16 cceff^2 cpc^2 cpeff^2 \\
 & - 32 cceff cpc^4 cpeff) cpp^2 + (-6 cceff^2 cpc^2 cpeff^3 - 28 cceff cpc^4 cpeff^2) \\
 & \left. cpp + cceff cpc^4 cpeff^3 + 4 cpc^6 cpeff^2 \right) / cceff) / (6 \sqrt{3} cceff) \\
 & + (cceff (-16 cpp^3 + 6 cpeff cpp^2 - 3 cpeff^2 cpp + 2 cpeff^3) \\
 & + cpc^2 (36 cpeff cpp + 9 cpeff^2)) / (54 cceff), \frac{1}{3}) - \frac{2 cpp - cpeff + 3 cpc}{3}
 \end{aligned}$$